



3-(*N*-Arylsulfamoyl)benzamides, inhibitors of human sirtuin type 2 (SIRT2)

Soo Hyuk Choi^{a,†}, Luisa Quinti^b, Aleksey G. Kazantsev^b, Richard B. Silverman^{a,*}

^aDepartments of Chemistry and Molecular Biosciences, Chemistry of Life Processes Institute, Center for Molecular Innovation and Drug Discovery, Northwestern University, Evanston, Illinois 60208-3113, United States

^bMassGeneral Institute for Neurodegenerative Disease, Massachusetts General Hospital and Harvard Medical School, 114 16th Street, Charlestown, MA 02129, United States

ARTICLE INFO

Article history:

Received 20 January 2012

Accepted 24 February 2012

Available online 3 March 2012

Keywords:

Sirtuin 2

Neurodegenerative disease

3-(*N*-Arylsulfamoyl)benzamides

Sirtuin selectivity

Hydrophobic pocket

ABSTRACT

Inhibition of sirtuin 2 (SIRT2) is known to be protective against the toxicity of disease proteins in Parkinson's and Huntington's models of neurodegeneration. Previously, we developed SIRT2 inhibitors based on the 3-(*N*-arylsulfamoyl)benzamide scaffold, including 3-(*N*-(4-bromophenyl)sulfamoyl)-*N*-(4-bromophenyl)benzamide (**C2-8**, **1a**), which demonstrated neuroprotective effects in a Huntington's mouse model, but had low potency of SIRT2 inhibition. Here we report that *N*-methylation of **1a** greatly increases its potency and results in excellent selectivity for SIRT2 over SIRT1 and SIRT3 isoforms. Structure–activity relationships observed for **1a** analogs and docking simulation data suggest that the *para*-substituted amido moiety of these compounds could occupy two potential hydrophobic binding pockets in SIRT2. These results provide a direction for the design of potent drug-like SIRT2 inhibitors.

© 2012 Elsevier Ltd. All rights reserved.

Sirtuin 2 (SIRT2), one of seven known human sirtuins, is a NAD⁺-dependent enzyme that catalyzes the deacetylation of histone and other substrate *N*^ε-acetyllysines with concomitant formation of nicotinamide and 2'-*O*-acetyl-ADP-ribose.¹ Previous studies showed that inhibition of SIRT2 mediated neuroprotective effects in Parkinson's disease (PD) and Huntington's disease (HD) models.^{2–4} In *in vitro* models of PD and HD, neuroprotective effects of SIRT2 inhibition have been associated with changes in aggregation of the α -synuclein and huntingtin proteins, respectively. A previously identified inhibitor of polyglutamine aggregation, a hallmark of many neurodegenerative diseases,⁵ namely **C2-8** (**1a**, Fig. 1), has potential as a therapeutic candidate based on its neuroprotective effects achieved in transgenic HD models and, apparently, good drug-like properties.⁶ **AK-1** (**1b**), which has a common 3-sulfobenzamide scaffold to that of **1a** and is neuroprotective against α -synuclein toxicity,² is a SIRT2 inhibitor that was reported to have good selectivity for SIRT2 over SIRT1 and SIRT3.² Most known SIRT2 inhibitors show low selectivities for SIRT1 and SIRT3, even though their potencies are better than that of **1b**.^{7–11} Compound **1a**, however, displayed low potency as a SIRT2 inhibitor. Here we test the feasibility of enhancing SIRT2 inhibition and selectivity of the therapeutically promising structural scaffold **1a**. We report the discov-

ery of more potent and highly selective SIRT2 inhibitors and describe related structure–activity relationship (SAR) studies.

Scheme 1 shows the structures of and related synthetic routes to analogs of **1a**. Compounds **2a–d** were prepared from 3-(chlorosulfonyl)benzoic acid (**5**) and the corresponding *para*-substituted anilines **6** in one step. Compounds **3a–e** and **4a** were prepared from **5** and **6** in two steps by consecutive amide coupling reactions. Compounds **4b–d** were synthesized from **1a** in one step by selective *N*-alkylation using potassium carbonate and the corresponding alkyl halide at 50 °C.

Figure 2 shows *in vitro* SIRT1, SIRT2, and SIRT3 inhibition assay results for **1a,b** and two *N*-methylsulfonamide analogs, **2a** and **4a**. Compound **1a** is a weaker SIRT2 inhibitor than **1b**, as reported previously.⁴ The potencies of **2a** and **4a** with SIRT2, however, are very similar and are slightly better than that of **1b**. In addition, **2a** and **4a** are more selective SIRT2 inhibitors than **1b**; **2a** and **4a** are virtually inactive with SIRT1 and SIRT3 up to 50 μ M, while **1b** shows some inhibitory activity with SIRT1. These results suggest that simple modifications of **1a** (methylation) can enhance both potency and selectivity toward SIRT2. A subsequent SAR study, changing the *para*-substituents (**2**) or the *N*-alkyl substituent (**4**), identified **2b** as a more potent SIRT2 inhibitor (see **Supplementary data Fig. S1**). Compound **2b** was selective for SIRT2; at 10 μ M concentration **2b** did not inhibit SIRT1 and inhibited SIRT3 by only 5% (see **Supplementary data Fig. S2**).

Further modification of the *para*-substituents (**3a–e**, **Table 1**) shows that two compounds, **3a** and **3e**, inhibit the SIRT2 activity by about half at 10 μ M concentration. Compounds **3a** and **3e** were highly selective; there was no inhibition of SIRT1 or SIRT3 at 10 μ M

Abbreviations: SIRT, sirtuin; PD, Parkinson's disease; HD, Huntington's disease; SAR, structure–activity relationship.

* Corresponding author. Tel.: 847 491 5653.

E-mail addresses: r-silverman@northwestern.edu, Agman@chem.northwestern.edu (R.B. Silverman).

[†] Current address: Department of Chemistry, Yonsei University, Seoul, South Korea.

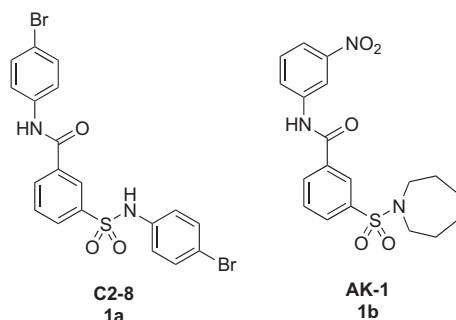
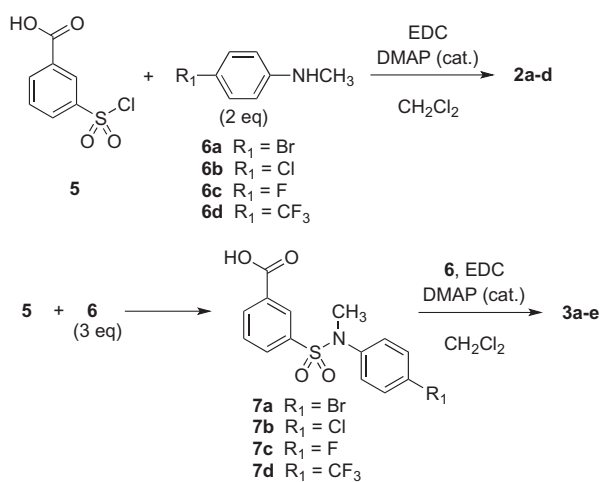
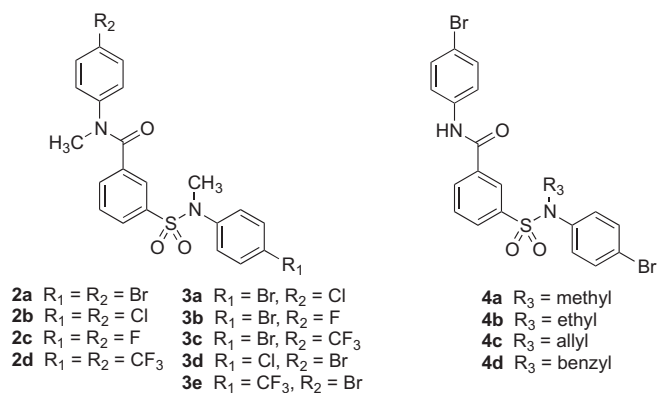


Figure 1. Structures of polyglutamine aggregation inhibitor **C2-8** (**1a**) and SIRT2 inhibitor **AK-1** (**1b**).



Scheme 1. Syntheses of **2-4**.

concentration. However, more extensive testing of **3a** and **3e**, such as a direct comparison of **3d** and **3e** as shown in Figure 3, confirmed **3a** to be a more potent SIRT2 inhibitor than **3e**. Compound **3a**, therefore, was selected for testing with **2a**, **2b**, and **1b** (Fig. 4). Figure 4 shows that all of these analogs of **1a** are more potent than **1b**. It should be noted that experiments represented by Figures 2 and 4 were carried out months apart, and the values differ somewhat. Compound **1b** was routinely included in assays for normalization of results.

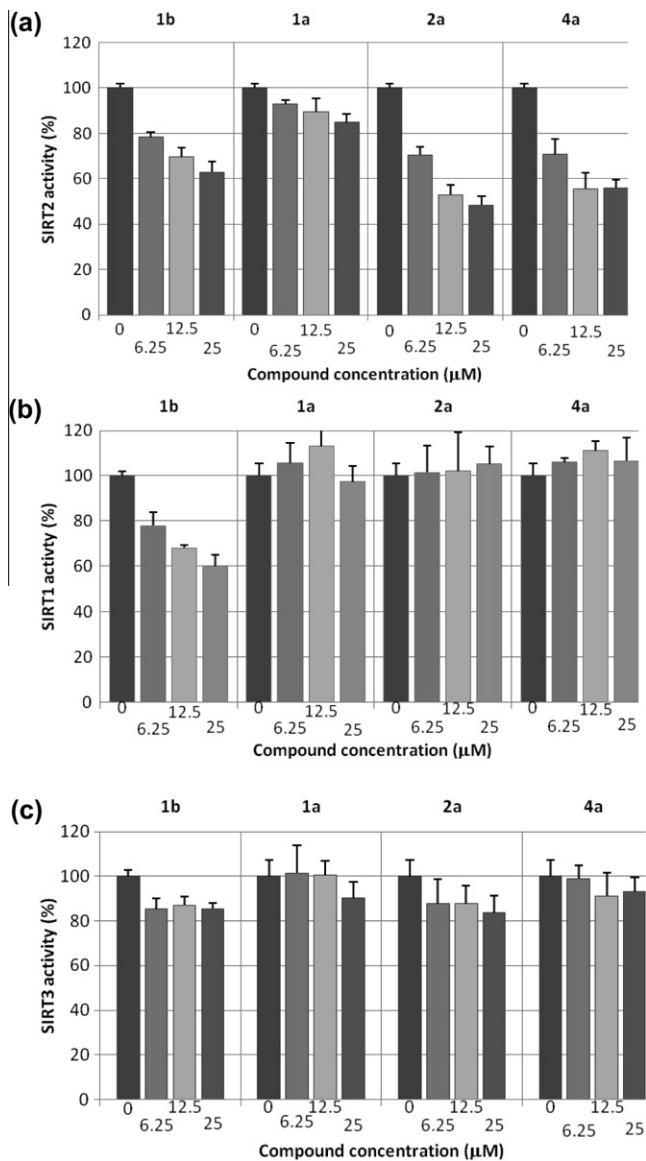


Figure 2. Compound inhibition activities in in vitro sirtuin-catalyzed lysine deacetylation assays. Potency and selectivity of **1a,b**, **2a**, and **4a** have been evaluated in dose-response assays against deacetylase activities of SIRT2, SIRT1, and SIRT3 at indicated concentrations. Each dose has been tested in triplicate. Compound **1b** was included as a reference compound.

Table 1
In vitro SIRT2 inhibition assay results for **3a-e**

Compound	Relative SIRT2 activity ^a (%)	Concentration of compounds (μM)
3a	54	10
3b	57	50
3c	76	50
3d	72	10
3e	55	10

^a Measured by the relative fluorescence observed from the SIRT2 assay.

To date, the only available crystal structure of SIRT2 does not contain any ligand molecule bound¹; it is likely that the uncomplexed SIRT2 structure is different from that of a ligand-bound conformation. A few computational methods have been reported to find the active conformation of SIRT2, including those that use energy minimization and/or molecular dynamics simulations^{9,12-14} and a homology model constructed from the SIRT2

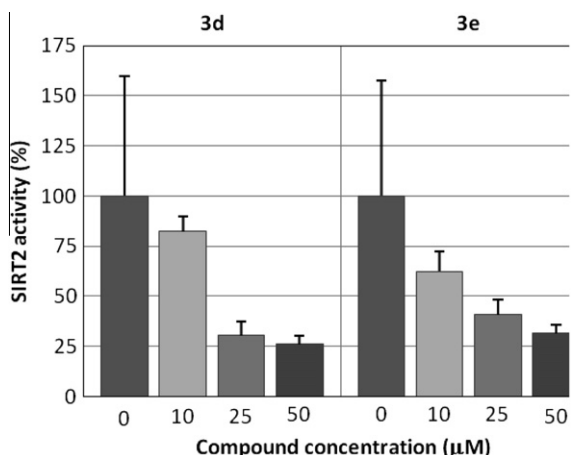


Figure 3. Comparison of SIRT2 dose–response activities for **3d** and **3e**.

structure and other homolog–ligand complex structures.^{2,15} The SIRT2 structure without any modification has been used in a few cases.^{10,16} We carried out docking simulations with the original crystal structure of SIRT2.¹ Although quantitative assessment

of binding interactions using a binding score would not be reliable, we assumed that at least a qualitative evaluation of binding conformations of analogs of **1a** with SIRT2 could be garnered. Figure 5(a) shows a putative ligand-binding site in SIRT2, proposed previously by a comparison with the crystal structures of other sirtuin homolog–ligand complexes.^{17–19} There are two potential hydrophobic binding pockets in the active site. A small cleft between Phe119 and His187 would be a good hydrophobic binding pocket for an aromatic ring, which could be stabilized by π – π interactions with the phenyl group of Phe119 and the imidazole ring of His187. This channel has been proposed as the binding site for the side chain of the acetylated lysine residue of a substrate. There is another potential hydrophobic binding pocket surrounded by residues with hydrophobic side chains Phe96, Tyr104, Leu107, Leu112, Pro115, Ile118, Phe119, Leu134, and Leu138. Docking simulation results predict that the two *para*-substituted anilino moieties of analogs of **1a** occupy the two potential hydrophobic pockets. Figure 5(b) shows a potential binding conformation for **4a**. The two *p*-bromophenyl groups are bound into the two hydrophobic pockets of SIRT2. Additionally, there is a hydrogen bond between the carbonyl group of **4a** and the hydroxyl group of Tyr104. Other active analogs of **1a** adopted very similar conformations in docking simulations.

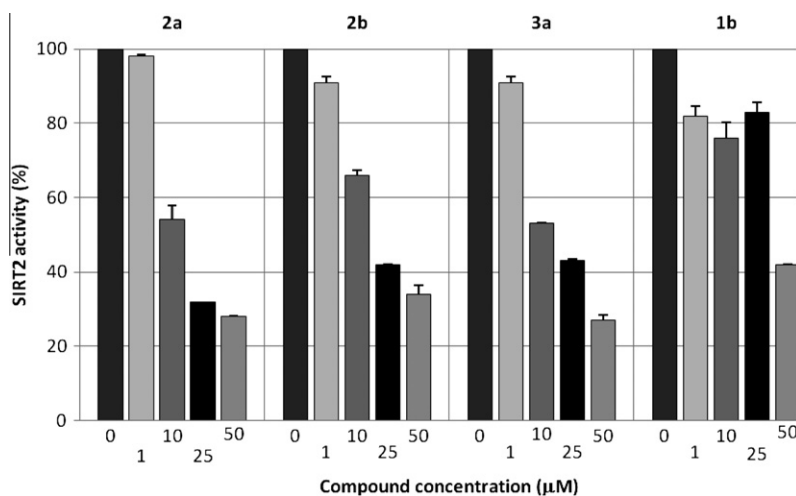


Figure 4. SIRT2 inhibition by three analogs of **1a** compared with that of **1b**.

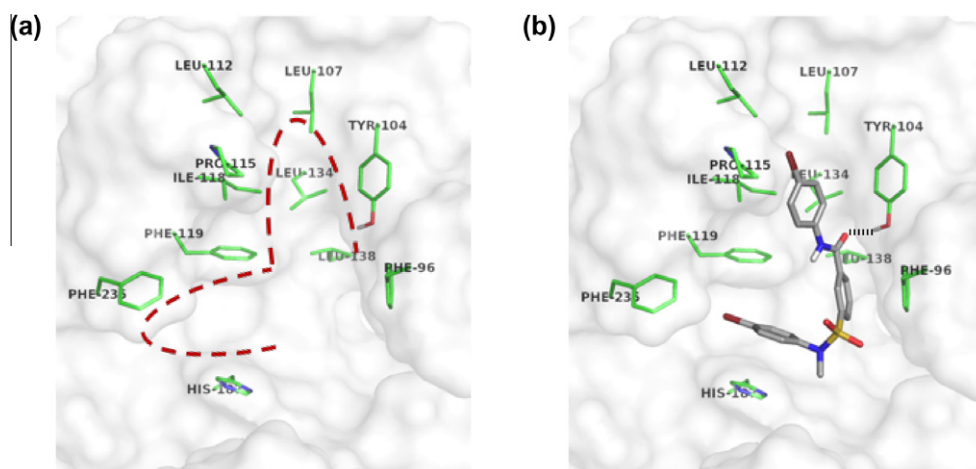


Figure 5. (a) Putative binding site of SIRT2; hydrophobic pockets are surrounded by a red dotted line. (b) Binding conformation of **4a** predicted by a docking simulation with a potential H-bond shown.

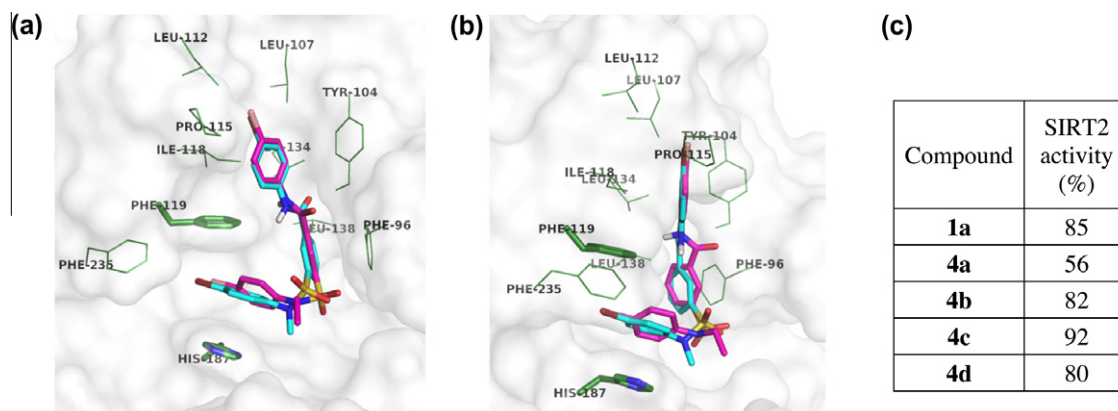


Figure 6. (a, b) Overlay of binding conformations of **4a** (cyan) and **4b** (magenta) from different views (c) Relative SIRT2 activity from treatment with **1a** and **4a–d** at 25 μ M.

The inhibitory assay data for **2a–d** and **3a–e** suggested that the potency might be correlated with the size of the two *para*-substituents, R_1 and R_2 (Scheme 1), both of which contribute to the hydrophobic interactions in the purported hydrophobic pockets. It is reasonable that there would be an optimal size for R_1 or R_2 that is dependent on the size of a hydrophobic binding pocket to maximize hydrophobic contact. Among the four compounds with the same R_1 group ($R_1 = \text{Br}$), **2a** ($R_2 = \text{Br}$), and **3a** ($R_2 = \text{Cl}$) showed comparable activities that were much higher than those of **3b** ($R_2 = \text{F}$) and **3c** ($R_2 = \text{CF}_3$). The order of van der Waals volumes for the four R_1 substituents is $\text{CF}_3 > \text{Br} > \text{Cl} > \text{F}$. It is therefore likely that the maximum hydrophobic contact might be achieved with an R_2 group having a van der Waals volume between Cl and Br. By the same analogy, the activities of the three compounds with the same R_2 group ($R_2 = \text{Br}$) can be compared to derive the optimal size for the R_1 group. The activity of **2a** ($R_1 = \text{Br}$) is greater than those of **3d** ($R_1 = \text{Cl}$) and **3e** ($R_1 = \text{CF}_3$), suggesting that the size of the hydrophobic binding pocket for the R_1 group might be similar to that of the R_2 -binding pocket.

Five analogs of **1a**, including **1a** and **4a–d**, contain the same R_1 and R_2 groups ($R_1 = R_2 = \text{Br}$) and are structurally different only by the R_3 substituent. Among these five compounds, only **4a** ($R_3 = \text{Me}$) showed significant activity against SIRT2, indicating that the *N*-methylsulfonamide moiety is crucial to the SIRT2 activity. Considering that the docked conformation of **1a** is very similar to that of **4a**, the increased potency of **4a** over **1a** could be attributed to the additional van der Waals contact between the *N*-methylsulfonamide moiety of **4a** and SIRT2. However, this one additional hydrophobic interaction should not be sufficient to explain the much greater potency of **4a**. One possible explanation is that the *N*-methyl substituent behaves as an anchor to direct the adjacent *para*-bromoanilino group close to the channel between Phe119 and His187, resulting in more favorable hydrophobic interactions.

Figure 6 shows two views of an overlay of the binding conformations of **4a** and **4b**. Although **4b** differs from **4a** by only one methylene unit, the *N*-ethylsulfonamide moiety of **4b** causes steric hindrance with SIRT2 and distorts the orientation of the adjacent *p*-bromoanilino group. The view in Figure 6(b) clearly shows that the *p*-bromophenyl ring at the sulfonamide moiety of **4b** is twisted out of plane for optimal π – π interactions with Phe119 and His187, while the corresponding *p*-bromophenyl ring of **4a** is aligned parallel to Phe119 and His187. The R_3 groups of **4c** and **4d** would cause even larger steric hindrance with SIRT2, rationalizing their lower potencies. In contrast to the *N*-substituent of the sulfonamide moiety, the *N*-substituent of the amide moiety does not seem to affect the SIRT2 activity significantly; **2a** and **4a** had

comparable activities. The binding conformation of **4a** in Figure 6(b) shows that the proton of the amide moiety is exposed to solvent, suggesting that no significant binding interaction is contributed by the *N*-methylamide moiety of **2a**.

We have demonstrated that **1a** could serve as a lead scaffold for inhibitors of SIRT2. The *N*-methylsulfonamide moiety of analogs of **1a** increases both SIRT2 activity and selectivity, both of which are higher than the known SIRT2 inhibitor **1b**. The observed structure–activity relationships with various R_1 and R_2 groups are consistent with the binding conformation of analogs of **1a** predicted by docking simulations. Both terminal aniline moieties might occupy the two potential hydrophobic binding pockets having strict size requirements. These observed SARs should be valuable for structure-based design of more potent SIRT2 inhibitors.

Acknowledgment

The authors are grateful to the National Institutes of Health (5U01NS066912) for financial support of this research.

Supplementary data

Supplementary data (experimental procedures, in vitro SIRT2 inhibition data, NMR spectra, and HRMS data) associated with this article can be found, in the online version, at doi:10.1016/j.bmcl.2012.02.089.

References

- Finnin, M. S.; Donigian, J. R.; Pavletich, N. P. *Nat. Struct. Biol.* **2001**, *8*, 621.
- Outeiro, T. F.; Kontopoulos, E.; Altmann, S. M.; Kufareva, I.; Strathearn, K. E.; Amore, A. M.; Volk, C. B.; Maxwell, M. M.; Rochet, J. C.; McLean, P. J.; Young, A. B.; Abagyan, R.; Feany, M. B.; Hyman, B. T.; Kazantsev, A. G. *Science* **2007**, *317*, 516.
- Luthi-Carter, R.; Taylor, D. M.; Pallos, J.; Lambert, E.; Amore, A.; Parker, A.; Moffitt, H.; Smith, D. L.; Runne, H.; Gokce, O.; Kuhn, A.; Xiang, Z.; Maxwell, M. M.; Reeves, S. A.; Bates, G. P.; Neri, C.; Thompson, L. M.; Marsh, J. L.; Kazantsev, A. G. *Proc. Natl. Acad. Sci. U.S.A.* **2010**, *107*, 7927.
- Taylor, D. M.; Balabadra, U.; Xiang, Z.; Woodman, B.; Meade, S.; Amore, A.; Maxwell, M. M.; Reeves, S.; Bates, G. P.; Luthi-Carter, R.; Lowden, P. A.; Kazantsev, A. G. *ACS Chem. Biol.* **2011**, *6*, 540.
- Riley, B. E.; Orr, H. T. *Genes Dev.* **2006**, *20*, 2183.
- Zhang, X.; Smith, D. L.; Meriin, A. B.; Engemann, S.; Russel, D. E.; Roark, M.; Washington, S. L.; Maxwell, M. M.; Marsh, J. L.; Thompson, L. M.; Wanker, E. E.; Young, A. B.; Housman, D. E.; Bates, G. P.; Sherman, M. Y.; Kazantsev, A. G. *Proc. Natl. Acad. Sci. U.S.A.* **2005**, *102*, 892.
- Rotili, D.; Carafa, V.; Tarantino, D.; Botta, G.; Nebbioso, A.; Altucci, L.; Mai, A. *Bioorg. Med. Chem.* **2011**, *19*, 3659.
- Huhtiniemi, T.; Salo, H. S.; Suuronen, T.; Poso, A.; Salminen, A.; Leppänen, J.; Jarho, E.; Lahtela-Kakkonen, M. *J. Med. Chem.* **2011**, *54*, 6456.

9. Huber, K.; Schemies, J.; Uciechowska, U.; Wagner, J. M.; Rumpf, T.; Lewrick, F.; Süß, R.; Sippl, W.; Jung, M.; Bracher, F. *J. Med. Chem.* **2010**, *53*, 1383.
10. Medda, F.; Russell, R. J.; Higgins, M.; McCarthy, A. R.; Campbell, J.; Slawin, A. M.; Lane, D. P.; Lain, S.; Westwood, N. J. *J. Med. Chem.* **2009**, *52*, 2673.
11. Trapp, J.; Jochum, A.; Meier, R.; Saunders, L.; Marshall, B.; Kunick, C.; Verdin, E.; Goekjian, P.; Sippl, W.; Jung, M. *J. Med. Chem.* **2006**, *49*, 7307.
12. Neugebauer, R. C.; Uciechowska, U.; Meier, R.; Hruby, H.; Valkov, V.; Verdin, E.; Sippl, W.; Jung, M. *J. Med. Chem.* **2008**, *51*, 1203.
13. Kiviranta, P. H.; Salo, H. S.; Leppanen, J.; Rinne, V. M.; Kyrlylenko, S.; Kuusisto, E.; Suuronen, T.; Salminen, A.; Poso, A.; Lahtela-Kakkonen, M.; Wallen, E. A. *Bioorg. Med. Chem.* **2008**, *16*, 8054.
14. Tervo, A. J.; Kyrlylenko, S.; Niskanen, P.; Salminen, A.; Leppanen, J.; Nyronen, T. H.; Jarvinen, T.; Poso, A. *J. Med. Chem.* **2004**, *47*, 6292.
15. Trapp, J.; Meier, R.; Hongwiset, D.; Kassack, M. U.; Sippl, W.; Jung, M. *Chem. Med. Chem.* **2007**, *2*, 1419.
16. Kiviranta, P. H.; Leppanen, J.; Kyrlylenko, S.; Salo, H. S.; Lahtela-Kakkonen, M.; Tervo, A. J.; Wittekindt, C.; Suuronen, T.; Kuusisto, E.; Jarvinen, T.; Salminen, A.; Poso, A.; Wallen, E. A. *J. Med. Chem.* **2006**, *49*, 7907.
17. Hawse, W. F.; Hoff, K. G.; Fatkins, D. G.; Daines, A.; Zubkova, O. V.; Schramm, V. L.; Zheng, W.; Wolberger, C. *Structure* **2008**, *16*, 1368.
18. Hoff, K. G.; Avalos, J. L.; Sens, K.; Wolberger, C. *Structure* **2006**, *14*, 1231.
19. Avalos, J. L.; Bever, K. M.; Wolberger, C. *Mol. Cell* **2005**, *17*, 855.